

# Refinement of Ferrite Grain Size Near to the Ultra-Fine Range by Single-Pass and Multi-Pass Thermo-Mechanical Compression

D. Chakrabarti<sup>1,\*</sup>, S. Patra<sup>1</sup>, A. Haldar<sup>2</sup>, Vinod Kumar<sup>3</sup>

<sup>1</sup>Department of Metallurgical and Materials Engineering, Indian Institute of Technology (I.I.T.), Kharagpur, West Bengal 721 302, India

<sup>2</sup>Steel Metallurgy Division, Swinden Technology Centre, Tata Steel Europe, Moorgate Rotherham, UK

<sup>3</sup>R&D Centre for Iron and Steel, RDCIS, SAIL, Ranchi

**Abstract** Single-pass and multi-pass deformation schedules have been applied to low-C microalloyed steel containing Nb, Ti and V. Heavy deformation (~80%) in a single pass, just above or below the austenite-to-ferrite transformation temperature ( $A_{F3}$ ), followed by slow-cooling (@ 1°C/s) of the samples to room temperature, resulted in the formation of ultra-fine ferrite grain structures with average grain size of ~2 to 3  $\mu\text{m}$ . Ferrite grain size variation observed in the ultra-fine grained steel can be explained in view of several metallurgical phenomena such as, static and dynamic strain-induced austenite ( $\gamma$ )  $\rightarrow$  ferrite ( $\alpha$ ) transformation, dynamic recovery, dynamic recrystallisation, and grain-growth of ferrite. Multi-pass deformation schedule can also refine the ferrite-grain size close to the ultra-fine range (~3  $\mu\text{m}$ ) provided more than 50% reduction is applied in the finishing stage, between  $A_{F3}$  and  $A_{F2}$  temperatures.

**Keywords** Ultra-Fine Grain, Single-Pass, Multi-Pass Deformation, Plane-Strain Compression, Ferrite Grain Size, Grain Size Variation, Micro-Texture

## 1. Introduction

Beneficial effect of ferrite grain refinement on improving the strength and toughness of low-carbon steel is well established and that was the drive behind the industrial development of thermo-mechanical controlled processing (TMCP) of microalloyed steels, containing Nb, Ti and V[1]. Application of advanced TMCP refined the ferrite grain size down to the ultra-fine range ( $\leq 3 \mu\text{m}$ )[2-4]. The effects of prior austenite ( $\gamma$ ) grain size, deformation temperature ( $T_{\text{def}}$ ), true strain ( $\epsilon$ ), strain rate ( $\dot{\epsilon}$ ), and cooling rate (CR) on the formation of ultra-fine ferrite (UFF) grains, in low-carbon steels, have been studied extensively [2-9]. Use of finer  $\gamma$ -grain sizes (14-20  $\mu\text{m}$ ), large strain deformation ( $\epsilon > 0.5$ ) just above the  $A_{F3}$  temperature (750-850°C) at a high strain rate ( $>0.1/\text{s}$ ), followed by rapid cooling (CR  $> 30^\circ\text{C/s}$ ) of the samples can achieve homogeneous distribution of UFF grains through dynamic strain induced austenite ( $\gamma$ )  $\rightarrow$  ferrite ( $\alpha$ ) transformation, DSIT [2-9]. In an industrial rolling mill, the application of single and heavy deformation pass at a low temperature, with high and fast CR, is however, difficult due to the requirement of excessive rolling load (resulted

from the high material flow-stress), precise temperature control, and water-cooling unit [2]. Therefore, single-pass, as well as multi-pass deformation schedules has been performed in the present study, keeping the total deformation same, and the samples were cooled down at a slow-rate (1°C/s). The average ferrite grain size, grain size distribution, nature and distribution of the second phase and texture developed in both the schedules have been compared. Fine-scale grain size variation observed in the ultra-fine grain structures has also been studied as this aspect is yet to be understood fully.

## 2. Experimental Details

Plane-strain compression testing has been carried out on the samples (10×15×20 mm rectangular blocks) of a Nb-Ti-V microalloyed steel, Table 1, using the Gleeble®3500® simulator. Single-pass and multi-pass deformation schedules, having different amount of roughing, intermediate and finishing deformation passes have been applied at different temperatures, varying between 1050°C and 650°C. Schematic of a typical single pass deformation schedule is shown in Fig. 1, where the deformed samples were soaked at 1200°C, cooled at 1°C/s to the deformation temperature and either water-quenched or continued to cool down at a slow-rate (1°C/s) after the compression. Total amount of reduction (~80%) remained the same. Samples

\* Corresponding author:

debalay@metal.iitkgp.ernet.in (D. Chakrabarti)

Published online at <http://journal.sapub.org/ijmee>

Copyright © 2013 Scientific & Academic Publishing. All Rights Reserved

have been prepared for the metallographic studies and investigated by optical microscope, scanning electron microscope (EBSD), transmission electron microscope (TEM) and electron backscattered diffraction analysis (EBSD).

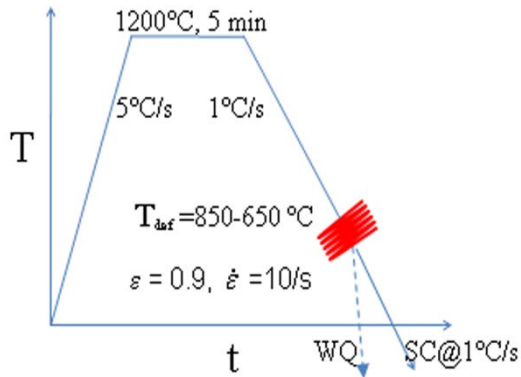


**Figure 1.** A single-pass, thermo-mechanical processing schedule performed in Gleeble®3500

**Table 1.** Chemical composition of the industrial slab (in wt %)

C	Si	Mn	P	S	Al	Nb	Ti	V	N
0.09	0.33	1.42	0.01 0	0.00 3	0.03 5	0.05 0	0.01 9	0.0 50	0.00 7

### 3. Results and Discussion

Applying heavy deformation in a single pass, just above the austenite-to-ferrite transformation temperature ( $A_{r3}$ ), followed by slow-cooling ( $@1^{\circ}\text{C/s}$ ) to the room temperature resulted in the formation of UFF grain structures, **Fig. 2**, with average  $\alpha$ -grain size between 2 and 3  $\mu\text{m}$  and the largest grain sizes extending up to  $\sim 10$  to 12  $\mu\text{m}$ . Water quenching just after deformation prevented the coarsening of UFF grains, offered finer average grain size ( $<2 \mu\text{m}$ ), and restricted the largest grain sizes to under 6  $\mu\text{m}$ [10]. Although the ferrite grain structures appeared homogeneous in slowly cooled samples, careful observation revealed the presence of alternate bands of coarse- (5 to 10  $\mu\text{m}$ ) and fine- $\alpha$  grains ( $<1$  to 3  $\mu\text{m}$ )[10].

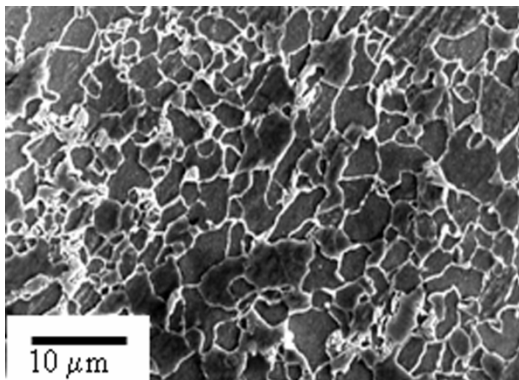


**Figure 2.** SEM micrograph of the sample deformed at 800°C showing the ultra-fine ferrite grain structure

The final  $\alpha$ -grain size distributions can be explained in view of the starting  $\gamma$ -grain size variation, static and dynamic strain-induced  $\gamma$ -to- $\alpha$  transformation (DSIT), dynamic recovery, recrystallisation (DRX), and grain growth of  $\alpha$  during slow cooling. For coarse  $\gamma$ -grains, higher strain accumulation near the  $\gamma$ -grain boundaries resulted in DSIT at those regions at a lower applied strain than at the  $\gamma$ -grain centre regions, **Fig. 3(a, b)**.

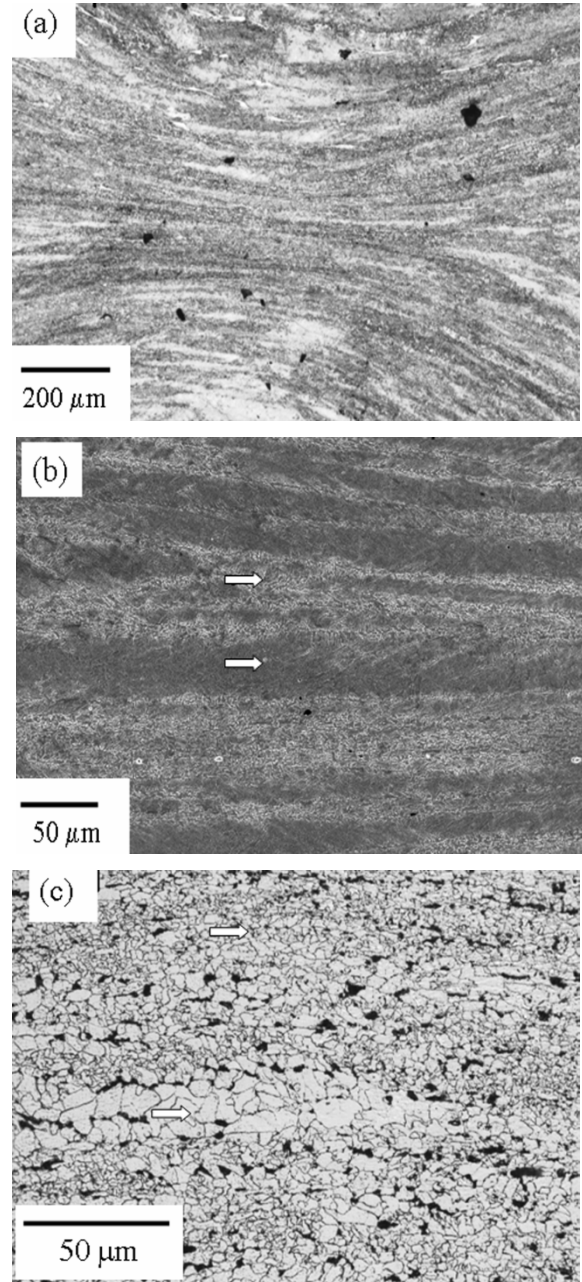


**Figure 3.** (a and b) Deformed region of the compression tested sample showing the formation of UFF grains along the prior- $\gamma$  grain boundaries; (c) After slow cooling, prior- $\gamma$  grain centre turned into lens-shaped coarse- $\alpha$  grain regions, which were surrounded by the UFF grains formed along the  $\gamma$ -grain-boundary regions. The prior- $\gamma$  grain-boundary and grain-centre regions are indicated by arrows

Three-dimensional impingement (i.e. impingement from all sides) of the  $\alpha$ -grains nucleated at the  $\gamma$ -grain-boundaries

prevented their growth and restricted those grains to below  $\sim 2 \mu\text{m}$ , even in case of slow cooling after deformation[9]. Upon further straining, at the later stage of deformation, DSIT can start on intra-granular defects at the  $\gamma$ -grain interior. Lack of impingement between those  $\alpha$ -grains can lead to grain-growth and the formation of closely spaced, parallel planar arrays (known as ‘rafts’) at the  $\gamma$ -grain centre regions. Due to the two-dimensional impingement, the grains in the raft can grow along the direction of the raft. Slow cooling of the samples subsequent to deformation, promotes the formation of carbide banding (perpendicular to the direction of compression) utilizing the carbon rejected during transformation[9, 10]. Carbide bands can also restrict the lateral growth of  $\alpha$ -grains and allows the  $\alpha$ -grains to grow along the direction of the raft. If the applied strain is insufficient to penetrate DSIT within the  $\gamma$ -grain interior,  $\gamma$ -grain centre regions may also transform statically, forming coarser  $\alpha$ -grains, surrounded by UFF grains developed at the  $\gamma$ -grain boundary regions. Statically transformed coarse  $\alpha$ -region is indicated in **Fig. 3c** and the ferrite-raft is indicated in **Fig. 4**. The distribution of  $\alpha$ -grain sizes becomes more uniform with the increase in applied strain and the decrease in prior  $\gamma$ -grain size, which resulted in the occurrence of DSIT in a more uniform fashion and distribute the carbide particles more uniformly throughout the structure[10]. Uniform distribution of carbide particles is beneficial for the grain size uniformity, as carbides prevent the  $\alpha$ -grain growth by pinning down the grain boundaries[4-10].

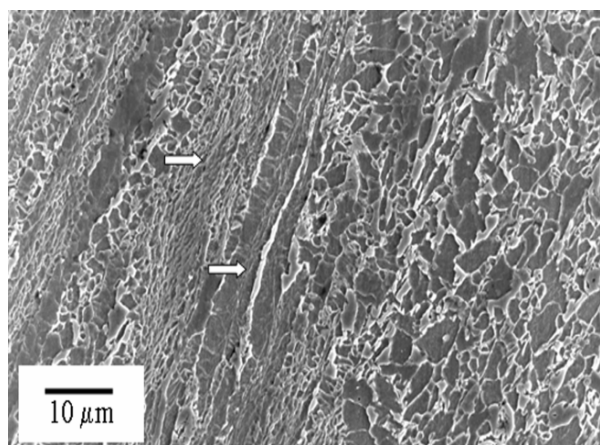


**Figure 4.** Ferrite grain size variation observed in the inter-critically deformed (at  $700^\circ\text{C}$ ) and slowly cooled sample. Coarse-grain raft and fine-grain region is arrowed and the arrows are along the direction of compression of the sample

Grain size variation may also arise after inter-critical deformation due to the recovery / recrystallisation of the deformed, pro-eutectoid ferrite and the dynamic / static transformation of the austenite. As ferrite and austenite co-deform, being the softer phase  $\alpha$  is deformed preferentially. Due to its high stacking fault energy ferrite has a tendency to recover dynamically, which promotes further strain accumulation in ferrite. Strain partitioning between  $\gamma$  and  $\alpha$  can influence the dynamic softening

behaviour of those phases and the resultant grain size variation. Microalloy precipitates also play a vital role in this aspect by retarding the dynamic recrystallisation of  $\gamma$  and  $\alpha$ , which alters the strain-partitioning and the resultant, dynamic softening.

Heavy finishing deformation (true strain  $\sim 0.8$ -1.0) between  $A_{e3}$  and  $A_{e1}$  using multiple-passes (for 10 s inter-pass time) effectively refined the ferrite ( $\alpha$ ) grain sizes ( $4.1$ - $3.2 \mu\text{m}$ ) nearly to the ultra-fine range[11]. Increasing the finishing deformation and the decrease in the number of passes and inter-pass time were found to be beneficial for the ferrite grain refinement. Besides grain refinement, heavy finishing deformation reduced the intensity of microstructural banding, pearlite fraction in the microstructure, and the fraction of harmful ‘cube’ texture component (to below 5%). Simultaneously, the fraction of small  $\text{Fe}_3\text{C}$  particles ( $50$ - $600 \text{ nm}$  size), high-angle ( $>15^\circ$  misorientation) boundaries (75-80%), beneficial  $\gamma$ -fibre ( $\langle\text{ND}\rangle/\langle 111 \rangle$ ) components and  $\{332\}\langle 113 \rangle$  and  $\{554\}\langle 225 \rangle$  texture components (40-45%) and the hardness of the deformed samples (184-192 HV) have been increased[11].

## 4. Conclusions

Major conclusions derived from the present investigation are summarized below:

- Single pass or multi-pass deformation refined the ferrite grain size nearly to the ultra-fine range ( $\sim 3 \mu\text{m}$  or below), when heavy deformation (true strain,  $\epsilon > 0.8$ ) has been applied between  $A_{e3}$  and  $A_{e1}$  temperatures.
- Fine-scale ferrite grain size variation remains even in the ultra-fine grain structures due to the dynamic  $\gamma \rightarrow \alpha$  transformation (DSIT) preferentially along the  $\gamma$  grain boundaries, whilst,  $\gamma$ -grain centre regions transform statically.
- Different rate of  $\alpha$ -nucleation and  $\alpha$ -grain growth between  $\gamma$ -grain boundary (high nucleation and stronger impingement) and  $\gamma$ -grain centre may also create a grain size variation after DSIT.
- Inter-critical deformation can also create ferrite grain size variation due to the extended dynamic recovery of ferrite grains and static transformation of austenite.

## ACKNOWLEDGEMENTS

Authors acknowledge Department of Science and Technology, New Delhi and Tata Steel, Jamshedpur, for the research funding and I.I.T. Kharagpur, Tata Steel and RDCIS, SAIL for the provision of research facilities.

## REFERENCES

- [1] T. Gladman: 'The Physical Metallurgy of Microalloyed Steels'; Book 615, The Institute of Materials, London, 1997, pp. 80-115.
- [2] R. Song, D. Ponge, D. Raabe, J.G. Speer, and D.K. Matlock: *Mat. Sci. and Engg. A*, 2006, 441, pp. 1-17.
- [3] R. Priestner and A. K. Ibraheem: *Mater. Sci. Technol.*, 2000, vol. 16, pp. 1267-1272.
- [4] P. D. Hodgson, M.R. Hickson, and R.K. Gibbs: *Scripta Mater.*, 1999, vol. 40, pp. 1179-1184.
- [5] H. Beladi, G.L. Kelly, and P.D. Hodgson: *Metall. Mater. Trans. A*, 2007, vol. 38A, pp. 450-63.
- [6] K. Mukherjee, S.S. Hazra, and M. Militzer: *Metall. Mater. Trans. A*, 2009, vol. 40A, pp. 2145-59.
- [7] P.R. Rios, I. de, S. Bott, D.B. Santos, T.M.F. de Melo, and J.L. Ferreira: *Mater. Sci. Technol.*, 2007, vol. 23 (4), pp. 417-22.
- [8] B. Eghbali and A. Abdollah-zadeh: *Scripta Mater.*, 2006, vol. 54, pp. 1205-09.
- [9] H. Beladi, G.L. Kelly, A. Shokouhi, and P.D. Hodgson: *Mater. Sci. Eng. A*, 2004, vol. 371, pp. 343-52.
- [10] S. Patra, S. Roy, Vinod Kumar, A. Haldar, and D. Chakrabarti: *Metall. Mater. Trans. A*, 2011, vol. 42, 2575-2590.
- [11] S. Patra, S. Neogi, Vinod Kumar, D. Chakrabarti, A. Haldar: Accepted in *Metall. Mater. Trans. A*, 2012.